NUMERICAL BUCKLING ANALYSIS OF LAMINATED COMPOSITE WING-SHAPED PLATES WITH BOX-TYPE STIFFENERS UNDER UNIFORM COMPRESSION

PHÂN TÍCH SỐ ỔN ĐỊNH CỦA TẤM COMPOSITE NHIỀU LỚP DẠNG CÁNH MÁY BAY VỚI GÂN HỘP DƯỚI TÁC DỤNG CỦA TẢI NÉN ĐỀU

Bui Van Binh
Electric Power University
Email: binhbv@epu.edu.vn

ABSTRACT

Composite wing-shaped plates reinforced with box-type stiffeners offer superior damage tolerance and high impact energy absorption. Due to their numerous advantages, the effect of geometric shapes, fiber orientation, and material properties on the buckling resistance of such structures remains a subject of continuing research interest among many scientists. This study performs a numerical buckling analysis of such structures using a finite element approach based on Reissner–Mindlin plate theory. The home-made Matlab programming using rectangular eight-noded isoparametric plate elements with five degrees of freedom per node was built to compute linear buckling loads and corresponding mode shapes.

Keywords: *Composite wing-shaped plates; Box-type stiffeners; Linear buckling; Reissner–Mindlin plate theory.*

TÓM TẮT

Tấm composite dạng cánh máy bay được gia cường bằng các gân hình hộp thể hiện khả năng chịu hư hỏng vượt trội và khả năng hấp thụ năng lượng va đập cao,... Chính vì có nhiều ưu điểm nên ảnh hưởng của hình dạng hình học, góc sợi và đặc tính vật liệu đến khả năng chịu mất ổn định của các kết cấu này vẫn đang được quan tâm nghiên cứu của nhiều nhà khoa học. Nghiên cứu này thực hiện phân tích mất ổn định bằng phương pháp số đối với các kết cấu nói trên, dựa trên lý thuyết tấm Reissner–Mindlin với chương trình phần tử hữu hạn tự phát triển trên nền tảng Matlab. Mô hình sử dụng phần tử tấm đẳng tham số tám nút với năm bậc tự do tại mỗi nút để tính toán tải trọng mất ổn định tuyến tính và các dạng mất ổn định tương ứng.

Từ khóa: *Tấm composite dạng cánh máy bay; Gân gia cường dạng hộp; Ổn định tuyến tính; Lý thuyết tấm Reissner–Mindlin.*

1. INTRODUCTION

Fiber-reinforced composite plates have emerged as a class of advanced engineering materials due to their superior strength-to-weight ratio, excellent corrosion resistance, and outstanding mechanical performance. These characteristics have led to their widespread adoption in various engineering sectors, including aerospace, automotive, marine, and civil engineering. In aerospace applications in particular, composite wing-shaped plates reinforced with box-type stiffeners are extensively utilized in the construction of structural components such as aircraft wings, fuselage panels, and interior elements, contributing significantly to weight reduction, improved fuel efficiency, and enhanced overall structural performance.

To meet the increasing demand for lightweight and high-performance structures, substantial research has been devoted to the analysis of the mechanical behavior of composite and stiffened plates. A range of analytical and numerical methods has been developed to investigate their static, dynamic, and stability responses under various loading conditions and geometric configurations. These studies have provided valuable insights for the design and optimization of advanced composite structures.

Recent research has focused on different aspects of composite plate behavior. For instance, Zhao et al. [1] studied the buckling behavior of stiffened rectangular plates using the finite element method based on first-order shear deformation theory, highlighting the effect of stiffener layout, curvature, and fiber orientation. Shi et al. [2] investigated the influence of initial imperfections, impact loads, and torsional stiffness of stiffeners on the dynamic response of stiffened plates using an analytical approach based on large-deflection theory. Lijuan et al. [3] employed the variational asymptotic method to develop an equivalent model for analyzing the static and dynamic responses of hemispherical convex–concave composite plates, addressing the effect of laminate layup and geometric configuration. Mohamed et al. [4] used the energy principle and first-order shear deformation theory to formulate the governing equations for helicoidally laminated composite plates, emphasizing the roles of fiber orientation and material properties. Wang et al. [5] explored free vibration in stiffened plates with and without cutouts, applying Reissner–Mindlin and Timoshenko beam theories in combination with the Nitsche method for patch coupling. Pereira and Donadon [6] investigated static, vibrational, and aeroelastic behaviors of composite plates using the modified consistent element-free Galerkin method. Bera et al. [7] conducted a comparative buckling study using classical plate theory and various higher-order shear deformation theories to assess the performance of isotropic and orthotropic plates. Z. Jing et al. [8] proposed a three-dimensional buckling analysis of stiffened plates with complex geometries using the energy element method, demonstrating its flexibility and accuracy.

Despite these advances, studies focusing on the compressive buckling behavior of wing-shaped laminated composite plates with integrated box-type stiffeners remain limited. This research gap is particularly evident in the Vietnamese academic context. To address this, the present study conducts a comprehensive numerical investigation on the linear buckling behavior of wing-shaped laminated composite plates reinforced with box-type stiffeners. The analysis systematically examines the effect of geometric parameters, material properties, and fiber orientation angles on the critical buckling loads and associated mode shapes. A finite element model based on Reissner–Mindlin plate theory is developed to perform the analysis. The outcomes of this study are expected to contribute to the structural design and optimization of lightweight composite components for aerospace applications.

2. FORMULATION OF THE PROBLEM

2.1. The strain-displacement relations

According to the Reissner-Mindlin plate theory [9], the displacements (u, v, w) are referred to those of the mid-plane (u_0, v_0, w_0) as:

$$\begin{aligned} u(x,y,z,t) &= u_0(x,y,t) + z\theta_x(x,y,t) \\ v(x,y,z,t) &= v_0(x,y,t) + z\theta_y(x,y,t) \\ w(x,y,z,t) &= w_0(x,y,t) \end{aligned} \quad (1)$$

Here, t is time, θ_x and θ_y are the total rotations, ϕ_x and ϕ_y are the constant average shear deformations about the y and x-axes, respectively.

The z-axis is normal to the xy-plane that coincides with the mid-plane of the laminate positive downward and clockwise with x and y.

2.2. Finite element formulations

In laminated plate theories [9], the membrane {N}, bending moment {M} and shear stress {Q} resultants can be obtained by integration of stresses over the laminate thickness. The stress resultants-strain relations can be expressed in the form:

$$\begin{Bmatrix} \{N\} \\ \{M\} \\ \{Q\} \end{Bmatrix} = \begin{bmatrix} [A_{ij}] & [B_{ij}] & [0] \\ [B_{ij}] & [D_{ij}] & [0] \\ [0] & [0] & [F_{ij}] \end{bmatrix} \begin{Bmatrix} \{\varepsilon^0\} \\ \{\kappa\} \\ \{\gamma^0\} \end{Bmatrix} \quad (2)$$

Where:

$$\left([A_{ij}],[B_{ij}],[D_{ij}]\right) = \sum_{k=1}^{n} \int_{h_{k-1}}^{h_k} \left([Q'_{ij}]_k\right)(1,z,z^2)\,dz$$

(i, j = 1, 2, 6) (3)

$$[F_{ij}] = \sum_{k=1}^{n} f \int_{h_{k-1}}^{h_k} \left([C'_{ij}]_k\right)dz; \quad f = 5/6; \; i,j = 4,5 \quad (4)$$

n: Number of layers, h_{k-1}, h_k: The position of the top and bottom faces of the kth layer.

$[Q'_{ij}]_k$ and $[C'_{ij}]_k$: Reduced stiffness matrices of the kth layer (see [9]).

In the present work, eight nodded isoparametric quadrilateral element with five degrees of freedom per nodes is used. The displacement field of any point on the mid-plane given by:

$$\begin{aligned} &u_0 = \sum_{i=1}^{8} N_i(\xi,\eta).u_i\,;\; v_0 = \sum_{i=1}^{8} N_i(\xi,\eta).v_i\,;\; w_0 = \sum_{i=1}^{8} N_i(\xi,\eta).w_i\,; \\ &\theta_x = \sum_{i=1}^{8} N_i(\xi,\eta).\theta_{xi}\,;\; \theta_y = \sum_{i=1}^{8} N_i(\xi,\eta).\theta_{yi} \end{aligned} \quad (5)$$

Where: $N_i(\xi, \eta)$ are the shape function associated with node i in terms of natural coordinates (ξ, η).

The eigenvalue type of buckling equation can be expressed as in the following steps by dropping force terms and conceded to:

$$\left\{[K] + \lambda_{CR}[K_G]\right\}\left\{\Delta d\right\} = \{0\} \quad (6)$$

Where, $[K_G]$ is the geometric stiffness ☞

matrix; {Δd} is the displacement increment vector and λ_{CR} is the critical mechanical load at which the structure buckles; [M], [K] are the global mass matrix, stiffness matrix, respectively.

3. NUMERICAL RESULTS

3.1. The composite wing-shaped plate

Consider a composite wing-shaped plate is shown in Figure 1; the dimensions of W = 0.8(m), l_i = 0.15(m) and a = 0.045 (m); total thickness of t = 7.25(mm), tapered angles of φ = 30°, 40°, 45°. Laminated scheme of [θ°/-θ°/θ°/-θ°/θ°]. The plate subjected to a uniform knife-edge loading of q (N/m) along its edge of AB towards the direction of y-xis. Material properties given in Table 1, Table 2 and Table 3.

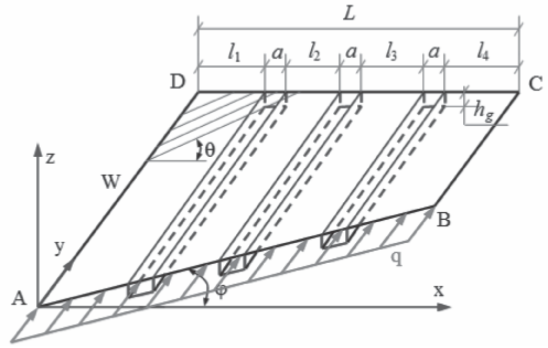

Figure 1. The composite wing-shaped plate with three box-type stiffeners under uniform compression

Table 1. Carbon fiber T700 material properties (MAT 1)

E_1 (GPa)	E_2, E_3 (GPa)	$G_{12, 13}$ (GPa)	G_{23} (GPa)	$\upsilon_{12,13}$	υ_{23}	ρ (kg/m³)
165	15	6.4	5.5	0.286	0.366	1611

Table 2. Woven fabric composite material properties (MAT 2)

E_1, E_2 (GPa)	E_3 (GPa)	$G_{12, 13,23}$ (GPa)	υ_{12}	υ_{13}	υ_{23}	ρ (kg/m³)
63.8	11.0	4.2	0.064	0.064	0.32	1523

Table 3. Graphite/epoxy AS4/3502 material properties (MAT 3)

E_1 (GPa)	E_2, E_3 (GPa)	G_{12} (GPa)	$G_{13,23}$ (GPa)	υ_{13}	$\upsilon_{12,23}$	ρ (kg/m³)
131	9.12	7.1	5.92	0.24	0.34	1600

Boundary conditions:

- At edge DC: u = v = w = θx = θy = θz = 0 (except stiffeners).

- At edges AD and BC: u = v = 0.

The non-dimensional buckling load parameter is defined as follows: $\lambda^*_{CR} = \dfrac{\lambda_{CR} L^2}{E_2 t^3}$.

3.2. Effect of taper angles

The geometric shape of the wing-shaped plate (taper angle) significantly influences the structural stability. In this subsection, to investigate the effect of taper angles on the buckling load, the laminated wing-shaped plates with laminated scheme of [45°/-45°/45°/-45°/45°] are considered for different taper angles of φ = 15°, 25°, 35°, 45°. The material properties shown in Table 1 (MAT 1); Comparative results corresponding to various taper angles are shown in Figure 2.

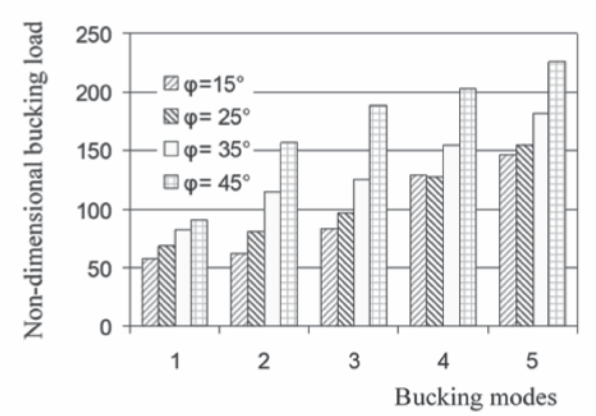

Figure 2. Effect of taper angles on buckling loads

The first five corresponding mode shapes with various taper angles of φ = 15°, 25°, 35°, 45° are shown in Figure 3-6.

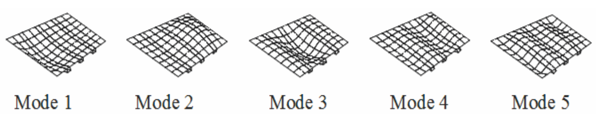

Figure 3. The first five mode shapes with taper angle of φ = 15°

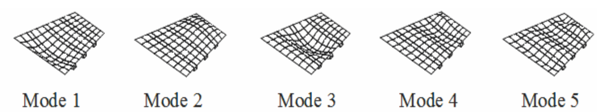

Figure 4. The first five mode shapes with taper angle of φ = 25°

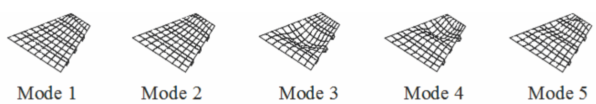

Figure 5. The first five mode shapes with taper angle of φ = 35°

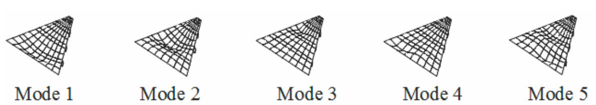

Figure 6. The first five mode shapes with taper angle of φ = 45°

The results shown in Figure 2 indicate that the non-dimensional buckling load of the laminated wing-shaped composite plates increases significantly when the taper angle φ increases from 15° to 45°, for all considered buckling modes (from mode 1 to mode 5). In particular, the plate with a taper angle of φ = 45° obtains the highest buckling loads in all modes, while the plate with φ = 15° gives the lowest values. This demonstrates that increasing the taper angle helps to improve the overall geometric stiffness of the plate, thereby enhancing its buckling resistance.

Moreover, the influence of the taper angle becomes more pronounced in higher buckling modes, as shown by the larger differences in buckling loads between different angles in mode 4 and mode 5. The nearly linear trend between buckling load and taper angle also suggests that the tapered geometry can be used as an effective design parameter to optimize the buckling performance of composite structures.

3.3. Effect of fiber orientations

To investigate the effect of fiber orientations on the buckling load, the composite plate with a taper angle of φ = 45° is considered for different fiber orientations of θ = 30°, 45°, 60°, 75° and laminated scheme of [0°/90°/0°/90°/0°] (denoted as [0°/90°/0°]s. Calculated buckling loads are compared in Figure 7.

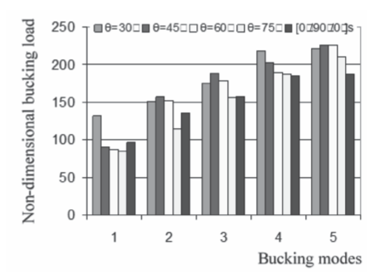

Figure 7. Effect of fiber orientations on buckling loads

The results presented in Figure 7 reveal that the buckling load is highly sensitive to the fiber orientation angle θ. Among the investigated cases, the fiber orientation of θ = 30° consistently provides the highest non-dimensional buckling loads, especially in buckling modes 3 and 5, indicating improved structural stability. In contrast, the fiber orientation of θ = 75° exhibits the lowest buckling capacities across all modes, reflecting reduced effectiveness in resisting buckling when fibers are aligned closer to the transverse direction. The symmetric laminated scheme [0°/90°/0°]s demonstrates relatively stable and moderate performance, offering balanced buckling resistance across different modes. Additionally, an increasing trend in buckling loads is observed with higher mode numbers for all fiber orientations, suggesting that the plate exhibits greater stiffness against higher-order buckling modes.

3.4. Effect of material properties

In this subsection, to investigate the effect of material properties on buckling loads, the laminated composite plate composed of three different materials (detailed in Tables 1, Tables 2, and Tables 3) with laminated scheme of [0°/90°/0°/90°/0°] and a taper angle of φ = 45° are considered. First five buckling loads calculated are compared in Figure 8.

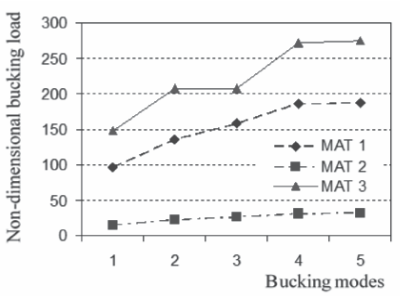

Figure 8. Effect of material properties on on buckling loads

The results presented in Figure 8 demonstrate a significant influence of material properties on the buckling performance of the composite plate. Among the three materials analyzed, MAT 3 consistently exhibits the highest non-dimensional buckling loads across all modes, indicating superior stiffness and stability characteristics. In contrast, MAT 2 yields the lowest buckling loads, suggesting it has the least effective mechanical properties for resisting buckling under the given configuration. MAT 1 shows intermediate performance, with buckling loads increasing steadily with the mode number. The results also reveal a clear trend of increasing buckling load with higher buckling modes for all materials, particularly notable in MAT 3, where a sharp increase is observed between modes 3 and 4. This indicates that the choice of material has a pronounced effect on both the magnitude and progression of buckling resistance across different modes.

4. CONCLUSIONS

This study has presented a numerical investigation on the linear buckling behavior of laminated composite wing-shaped plates reinforced with box-type stiffeners, based on a finite element formulation using Reissner–Mindlin plate theory. The effect of taper angle, fiber orientation, and material properties on the critical buckling load and corresponding buckling modes were systematically evaluated. From the numerical results, the following conclusions can be drawn:

- Taper angle significantly affects the structural stability of the composite plate. An increase in taper angle enhances the geometric stiffness, thereby increasing the critical buckling load across all mode numbers.

- Fiber orientation plays a crucial role in the buckling resistance. The fiber orientation of θ = 30° exhibited the highest buckling loads, while θ = 75° showed the lowest. The symmetric laminated scheme of [0°/90°/0°/90°/0°] provided balanced performance across different modes.

- Material properties strongly influence the buckling capacity. Among the three materials studied, MAT 3 demonstrated the highest stiffness and buckling resistance, while MAT 2 performed the weakest in terms of load-carrying capacity.

- For all considered parameters, higher-order buckling modes generally correspond to higher critical loads, emphasizing the role of structural stiffness and its sensitivity to design parameters.

The findings of this study provide useful insights into the design and optimization of lightweight composite wing structures, particularly in aerospace applications where stability under compressive loads is a key design requirement.❖

References:

[1]. W. Zhao, R. K. Kapania, "*Buckling analysis of unitized urvilinearly stiffened composite panels*". Composite Structures 135 (2016) 365-382.

[2]. Y. Xiong, G. Shi, F. Wang, D. Wang, "*Dynamic buckling analysis of stiffened panels under in-plane uniaxial impact considering plate/web interaction*". Ocean Engineering 279 (2023) 114462.

[3]. Z.Lijuan, Z. Yifeng, L. Qiushi, S. Zheng, "*Static and dynamic analysis of hemispherical convex-concave composite plate (HCCP) using variational asymptotic equivalent model*". Composite Structures 271 (2021) 114116.

[4]. S.A. Mohamed, N. Mohamed, M.A. Eltaher, "*Bending, buckling and linear vibration of bio-inspired composite plates*". Ocean Engineering 259 (2022) 111851.

[5]. Y. Wang, J. Fan, X. Shen, X. Liu, J. Zhang, N. Ren, "*Free vibration analysis of stiffened rectangular plate with cutouts using Nitsche based IGA method*". Thin-Walled Structures 181 (2022) 109975.

[6]. M. S. Pereira and M. V. Donadon, "*Modified consistent element-free Galerkin method applied to Reissner–Mindlin plates*". Thin-Walled Structures 212 (2025) 113185.

[7]. P. Bera, J. P. Varun, P. K. Mahato, "*Buckling analysis of isotropic and orthotropic square/rectangular plate using CLPT and different HSDT models*". Materials Today: Proceedings 56 (2022) 237-244.

[8]. Z. Jing, Y. Liu, L. Duan, S. Wang, "*Three-dimensional buckling analysis of stiffened plates with complex geometries using energy element method*". International Journal of Solids and Structures 306 (2025) 113105.

[9]. Decolon, C (2002), "*Analysis of Composite Structures*". Hermes Penton Ltd (English language edition).